Biochemical and Biophysical Research Communications 439 (2013) 453–458

Contents lists available at ScienceDirect

Biochemical and Biophysical Research Communications

journal homepage: www.elsevier.com/locate/ybbrc

Visualizing the effect of tumor microenvironments on radiation-induced cell kinetics in multicellular spheroids consisting of HeLa cells

Atsushi Kaida, Masahiko Miura *

Section of Oral Radiation Oncology, Department of Oral Health Science, Graduate School of Medical and Dental Sciences, Tokyo Medical and Dental University, 1-5-45 Yushima, Bunkyo-ku, Tokyo 113-8549, Japan

ARTICLE INFO

Article history:
Received 25 August 2013
Available online 7 September 2013

Keywords:
G2 arrest
Radiation
Fluorescent ubiquitination-based cell-cycle indicator (Fucci)
Spheroid
Tumor microenvironment

ABSTRACT

In this study, we visualized the effect of tumor microenvironments on radiation-induced tumor cell kinetics. For this purpose, we utilized a multicellular spheroid model, with a diameter of ~500 μm, consisting of HeLa cells expressing the fluorescent ubiquitination-based cell-cycle indicator (Fucci). In live spheroids, a confocal laser scanning microscope allowed us to clearly monitor cell kinetics at depths of up to 60 μm. Surprisingly, a remarkable prolongation of G2 arrest was observed in the outer region of the spheroid relative to monolayer-cultured cells. Scale, an aqueous reagent that renders tissues optically transparent, allowed visualization deeper inside spheroids. About 16 h after irradiation, a red fluorescent cell fraction, presumably a quiescent G0 cell fraction, became distinct from the outer fraction consisting of proliferating cells, most of which exhibited green fluorescence indicative of G2 arrest. Thereafter, the red cell fraction began to emit green fluorescence and remained in prolonged G2 arrest. Thus, for the first time, we visualized the prolongation of radiation-induced G2 arrest in spheroids and the differences in cell kinetics between the outer and inner fractions.

1. Introduction

Evidence is rapidly accumulating that tumor microenvironments, characterized by hypoxia, deficient nutrition, and low pH, exist in solid tumors, and that tumor cells often acquire therapeutic resistance under such conditions [1,2]. However, the effect of this tumor-specific milieu on cell kinetics still remains largely unknown, especially in the context of DNA damage. Although many researchers have attempted to elucidate cell kinetics in solid tumors following irradiation [2–4], direct analysis of detailed kinetics has proven technically challenging. Therefore, tumor-tissue models have been designed to compensate for the difficulty of analyzing cell kinetics in solid tumors [5]. Multicellular spheroids have frequently been used as models of solid tumors; in these systems, the three-dimensional anchorage-independent growth and the diffusion kinetics of oxygen and nutrients are thought to closely reflect tumor microenvironments *in vivo*[6–9].

Cell-cycle progression is regulated by cyclins and cyclin-dependent kinases (CDKs), and cell-cycle checkpoints are activated when DNA damage is induced during the cell cycle. Among several cell-cycle checkpoints [10], G2 arrest occurs in many types of tumor cells following irradiation, because normal p53 function is not necessarily required for G2 arrest [11–14]. In previous work, we succeeded in visualizing the radiation-induced G2 arrest kinetics in HeLa cells carrying non-functional p53 in monolayer conditions, using the fluorescent ubiquitination-based cell-cycle indicator (Fucci) [13–15]. Following irradiation, the number of cells expressing green fluorescence (normally expressed in S/G2/M phase) increased, whereas the number of cells expressing red fluorescence (normally expressed in G1 phase) almost disappeared, but subsequently returned to the basal level. In this study, taking advantage of Fucci, we directly observed the interiors of spheroids, consisting of HeLa cells expressing Fucci, by confocal laser scanning microscopy without histological preparation. The results provide the first clear demonstration that radiation-induced G2 arrest is remarkably prolonged in multicellular spheroids relative to monolayer-cultured cells.

2. Materials and methods

2.1. Cell culture and spheroid formation

HeLa cells expressing the Fucci probes (HeLa-Fucci) were provided by the RIKEN BRC through the National Bio-Resource Project of MEXT, Japan. Cells were maintained in DMEM (Sigma–Aldrich, St. Louis, MO) containing a high concentration of glucose (4500 mg/L) with 100 units/ml penicillin and 100 μg/ml streptomycin, supplemented with 10% fetal bovine serum (FBS), at 37 °C in a 5% CO_2 humidified atmosphere.

* Corresponding author. Fax: +81 3 5803 5897.
E-mail address: masa.mdth@tmd.ac.jp (M. Miura).

0006-291X/$ - see front matter © 2013 Elsevier Inc. All rights reserved.
http://dx.doi.org/10.1016/j.bbrc.2013.08.093

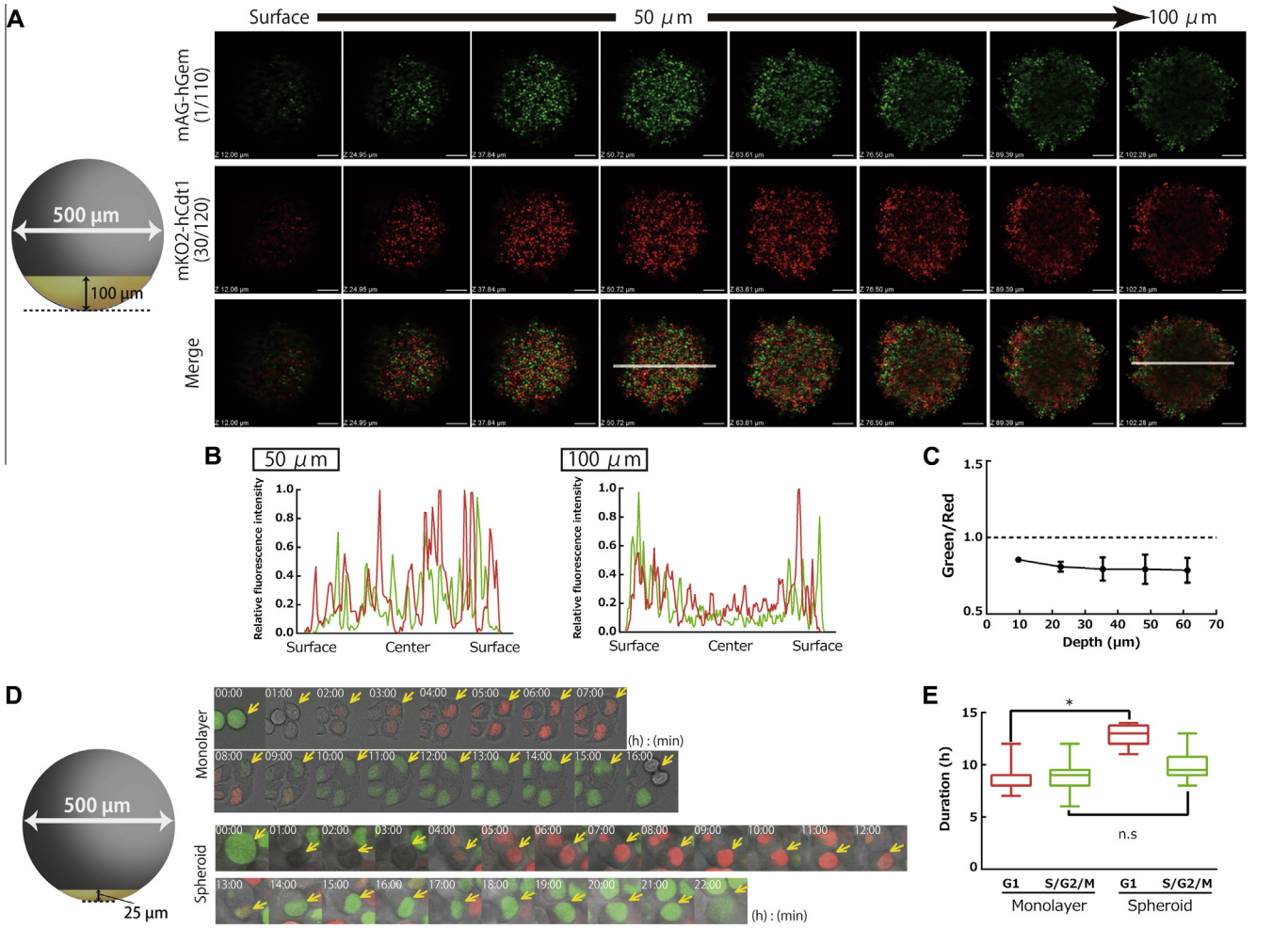

Fig. 1. Fluorescence distribution and cell-cycle kinetics in spheroids consisting of HeLa-Fucci cells. (A) Fluorescence images from the surface to a depth of 100 μm in a live spheroid with a diameter of ~500 μm. Scale bar, 100 μm. (B) Quantitative line-profile analysis of green and red fluorescence intensities at depths of 50 and 100 μm in a live spheroid. A line (white line) was drawn at each depth shown in Fig. 1A. Relative fluorescence intensity was normalized by adjusting the maximum fluorescence intensity to 1.0. Data shown are representatives of four spheroids. (C) Quantitative estimation of the ratio of the number of green cells to the number of red cells from the surface to a depth of 60 μm within the spheroid. The ratio was calculated by dividing the integrated green area by the integrated red area at each depth, and is plotted here as a function of the depth in the spheroid. The areas were quantitated using the ImageJ software (available from http://rsbweb.nih.gov/ij/). Data shown are represented as means ± SD. (D) Time-lapse imaging of fluorescence during the period of one cell cycle in HeLa-Fucci cells in monolayer culture and the spheroid. Time is shown as hours:minutes with a starting point at 00:00. (E) The duration of G1 or S/G2/M phases in live HeLa-Fucci cells in monolayer culture or the spheroid. The durations of G1 and S/G2/M were defined as the durations of the red and green phases, respectively. Data shown are represented as box-and-whisker plots showing the full range, 25–75% interquartile range (box), and median (bar) of G1 and S/G2/M phases of at least 20 cells. Median and 25% interquartile value of the duration of G1 phase in monolayer culture were the same. $^{*}p < 0.05$ versus the duration of each phase in HeLa-Fucci cells in monolayer culture. (For interpretation of the references to colour in this figure legend, the reader is referred to the web version of this article.)

A Hydrocell™ 24-well plate (CellSeed, Tokyo, Japan) was used to generate spheroids. Three thousand cells were plated onto each well and incubated for about 10 days. After the spheroids became visible to the naked eye during incubation, the culture medium was exchanged with fresh medium every 2 days. Spheroids about 500 μm in diameter were used in this study. In anchorage-independent cultures, 1×10^5 cells were plated onto a Hydrocell™ 6-cm dish (CellSeed, Tokyo, Japan) and irradiated after 24-h pre-culture.

2.2. Irradiation

Cells were irradiated at a dose of 10 Gy in an RX-650 Cabinet X-radiator system (Faxitron, Lincolnshire, IL) at a dose rate of 0.8 Gy/min. Parameters were set as follows: 130 kVp, 5 mA, 0.5 mm Al filtration.

2.3. Time-lapse imaging

For time-lapse imaging of spheroids, an FV10i-LIV confocal laser scanning microscope (Olympus, Tokyo, Japan) was equipped with two objective lenses (UPLSAPO 10×, NA = 0.4; UPLSAPO 60 × W, NA = 1.2). Each spheroid was prepared on a 35-mm glass-bottom dish coated with DMEM containing 0.5% agar so that the spheroid did not attach to the dish. To measure the duration of the cell cycle in HeLa-Fucci cells in spheroids, a high-power lens (UPLSAPO 60 × W, NA = 1.2) was used. For time-lapse imaging of monolayer-cultured cells, cells were also grown on a 35-mm glass-bottom dish, and images were taken using a BIOREVO BZ-9000 fluorescence microscope (KEYENCE, Osaka, Japan). During time-lapse imaging, both spheroids and cells were held in an incubation chamber at 37 °C in a humidified atmosphere containing 5% CO_2.

2.4. Flow-cytometric analysis

Two types of samples were subjected to flow-cytometric analysis: non-fixed samples, for detecting fluorescence intensity of mAG or mKO2, and fixed samples, for DNA-content analysis. Collected culture medium and trypsinized cells were centrifuged together at the indicated times after irradiation, and the pellets were

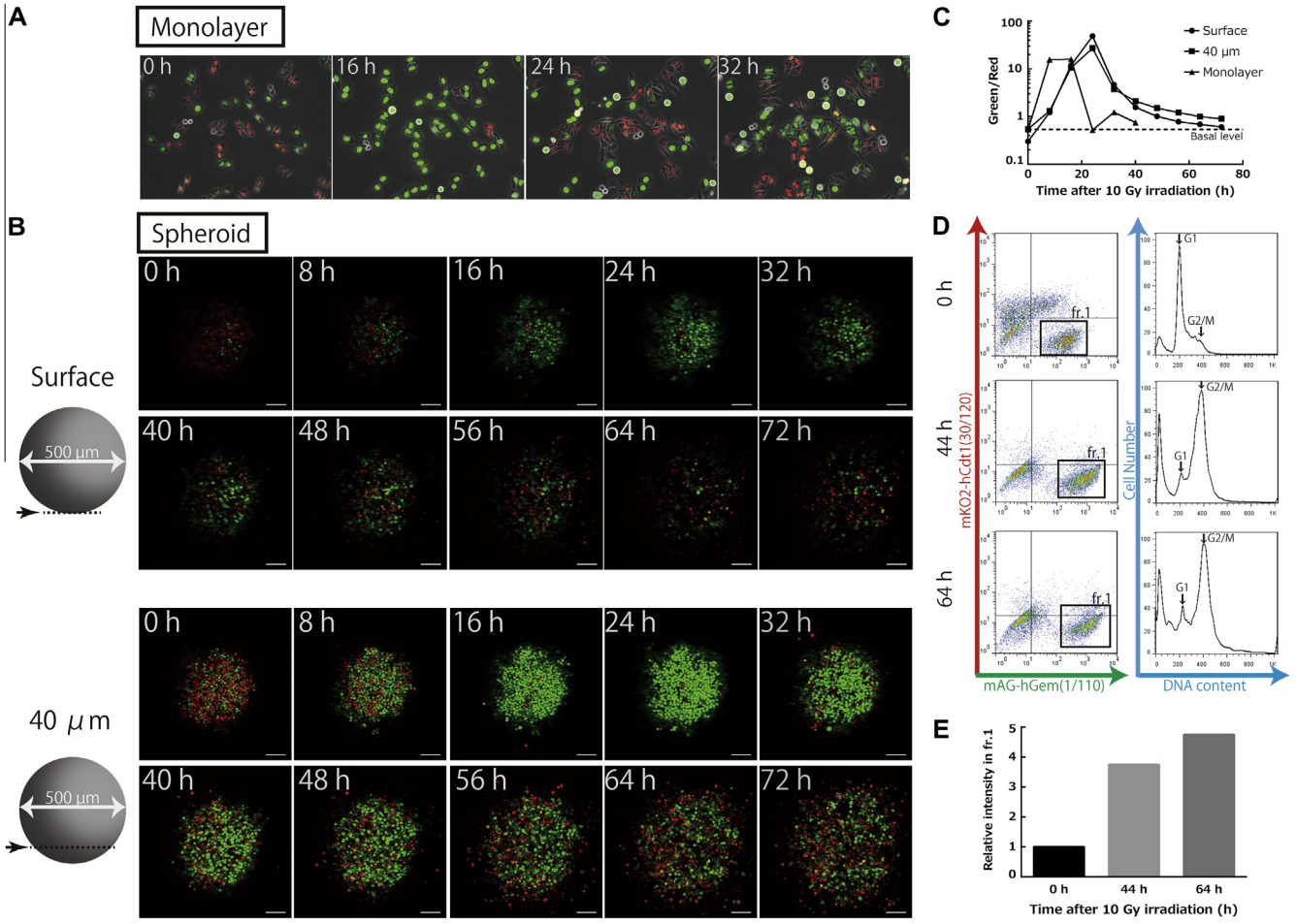

Fig. 2. Fluorescence kinetics in live HeLa-Fucci cells in monolayer culture and in outer regions of spheroids after irradiation. (A) Fluorescence images in monolayer culture at the indicated times after 10-Gy irradiation. (B) Fluorescence images at the surface and a depth of 40 μm at the indicated times after 10-Gy irradiation. All images were generated by time-lapse imaging. Images shown are representative of at least four experiments. Scale bar, 100 μm. (C) The ratio of the number of green cells to the number of red cells in monolayer culture and in outer regions of the spheroid after irradiation. The ratio was calculated in monolayer culture by dividing the number of green cells by the number of red cells, and in spheroids by dividing the green area by the red area, and is plotted here as a function of time after 10-Gy irradiation. Data shown here were representatives of four independent experiments. (D) Flow-cytometric analysis following 10-Gy irradiation. Left panels: histograms for two-dimensional (green and red fluorescence) analysis. Right panels: histograms for DNA-content analysis. Fr.1 indicates the fraction emitting only green fluorescence. Treated cells were trypsinized at the times indicated after 10-Gy irradiation and prepared for flow-cytometric analysis. Data shown here are representatives of two independent experiments. (E) Quantitative analysis of fr.1 in Fig. 2D. Data shown are the means of green fluorescence intensity in fr.1 from the two-dimensional analysis in Fig. 2D. (For interpretation of the references to colour in this figure legend, the reader is referred to the web version of this article.)

washed in ice-cold PBS. For DNA-content analysis, cells were fixed in ice-cold 70% ethanol in PBS for at least 30 min on ice. After fixation, cells were re-washed in ice-cold PBS and incubated in 0.5 μg/ml 7-AAD solution (BD Bioscience, San Jose, CA). Finally, both non-fixed and fixed single-cell suspensions were strained through nylon mesh. Each sample was analyzed using a FACScalibur flow cytometer (Becton Dickinson, Franklin Lakes, NJ) using the FlowJo software (Tree Star, Ashland, OR).

2.5. Scale treatment

Scale, an aqueous reagent that renders biological samples optically transparent, was developed to permit fluorescent imaging at deep positions within a tissue sample [16]. In this study, a SCALEVIEW-A2 solution (Olympus, Tokyo, Japan) was used to make spheroids more transparent. The solution was used as specified by the manufacturer. Briefly, spheroids at the indicated times after irradiation were fixed for 30 min in 4% paraformaldehyde (PFA) in 1 × PBS, and embedded in Tissue-Tek® OCT™ compound (Sakura Finetek, Tokyo, Japan) and stored at −80 °C overnight. Frozen spheroids were thawed and re-fixed in 4% PFA for 20 min, and then shaken for 10 days in SCALEVIEW-A2 solution at room temperature. The SCALEVIEW-A2 solution was exchanged with fresh solution every day. After this treatment, each spheroid was put onto a 35-mm glass-bottom dish to analyze fluorescence distribution. Imaging acquisition and analysis were performed using an FV10i-DOC confocal laser scanning microscope (Olympus, Tokyo, Japan) equipped with an objective lens (UPLSAPO 10×, NA = 0.4) and the FLUOVIEW software (Olympus, Tokyo, Japan).

2.6. Statistical analysis

The two-tailed *t*-test or Mann–Whitney *U* test was used for statistical determinations. *P* values <0.05 were considered statistically significant.

3. Results and discussion

3.1. Visualization and cell-kinetic characterization of live spheroids consisting of HeLa-Fucci cells

We examined fluorescence distribution in live spheroids consisting of HeLa-Fucci cells, using a confocal laser scanning micro-

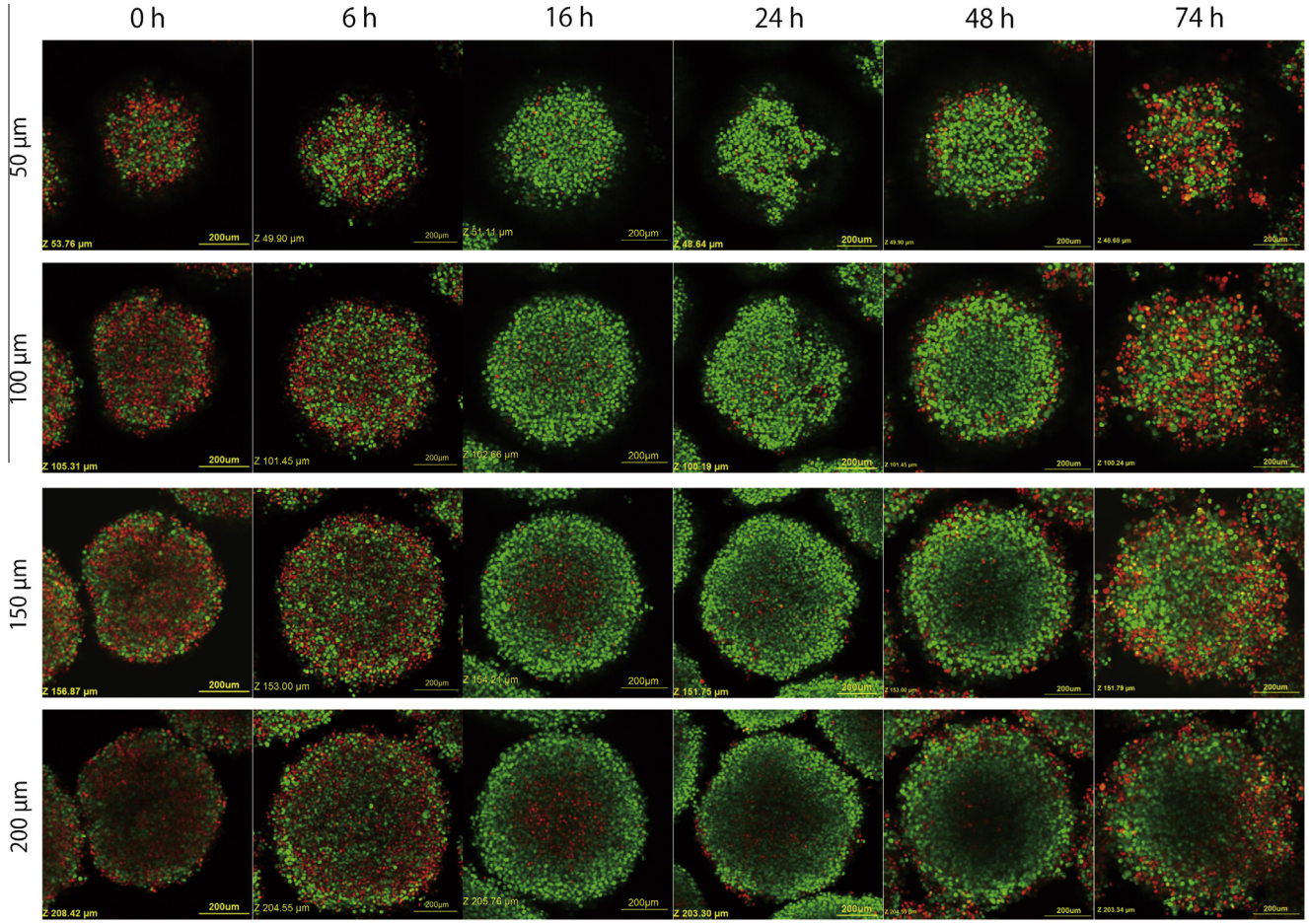

Fig. 3. Fluorescence distribution in Sca*l*e-treated spheroids after irradiation. Representative fluorescence images at depths of 50, 100, 150, and 200 μm in a Sca*l*e-treated spheroid at the indicated times after 10-Gy irradiation. Each spheroid was fixed and treated at the indicated times with Sca*l*e. Scale bar, 100 μm.

scope. Spheroids had diameters of ~500 μm. Fig. 1A shows green, red, and merged fluorescence images from the surface (bottom of the spheroid) up to a depth of 100 μm within the spheroid. Both red and green fluorescence were clearly detected even around the center of each confocal plane up to a depth of ~60 μm; however, at depths greater than 60 μm, the middle regions of each confocal plane were dark and no longer clearly identified, presumably due to the deterioration of optical conditions. Indeed, quantitative line-profile analysis of the fluorescence intensity revealed that values in the center areas at 100 μm depth were lower than those at 50 μm (Fig. 1B). Another quantitative analysis revealed that the ratio of green to red area was stable at ~0.8, irrespective of the depth up to 60 μm (Fig. 1C), demonstrating that there were no significant differences in localization of red and green cells up to a depth of 60 μm, although red area was stably higher. Furthermore, under this condition we could closely follow the change of fluorescent colors in each cell up to a depth of 25 μm, which for the first time allowed us to determine the cell-cycle duration in a live spheroid; the duration of the red phase (G1 phase) was significantly longer in the spheroid than in the monolayer condition, whereas the duration of the green phase (S/G2/M phases) was the same in both conditions (Fig. 1D and E).

3.2. Cell-cycle kinetics at outer positions in live spheroids after irradiation

We previously reported that fluorescence kinetics exactly reflect the radiation-induced G2 arrest kinetics in HeLa-Fucci cells in monolayer-culture conditions after 10 Gy irradiation [13,14]. In those studies, the number of green cells gradually increased and reached a peak 16 h after irradiation; subsequently, red cells appeared again, and returned almost to the basal level 24 h after irradiation. This temporal pattern was reproduced in this study (Fig. 2A). We then used time-lapse imaging to analyze cell-cycle kinetics in live spheroids at outer positions, surface and 40-μm depth, following 10-Gy irradiation. In general, cells at both depths exhibited similar kinetics: the number of green cells peaked 24 h after irradiation; thereafter, surprisingly, many cells in the spheroid maintained green fluorescence for a long time (Fig. 2B). Quantitative analysis revealed that the time required to reach the peak green/red ratio was delayed for a few hours, and the time required to return to the basal level after the peak was also delayed for more than 20 h relative to monolayer-cultured cells (Fig. 2C). The former delay in the spheroid could be explained by elongation of G1 phase, but the latter delay cannot be explained by a change in the cell-cycle time (Fig. 1E). We concluded that radiation-induced G2 arrest is prolonged in the spheroid.

This novel finding was further supported by several lines of evidence, as follows: (1) flow-cytometric analysis revealed persistence of the green cell fraction (fr.1 in Fig. 2D) accompanied by a decreased red cell fraction and increased G2/M fraction (as reflected by DNA) even 44 and 64 h after irradiation (Fig. 2D); (2) a higher intensity of green fluorescence in fr.1 at 44 and 64 h compared to 0 h after irradiation indicates that cells stayed in the green phase for a longer time, beyond the regular duration, because the Fucci probes are constantly being synthesized [15]; and (3) when

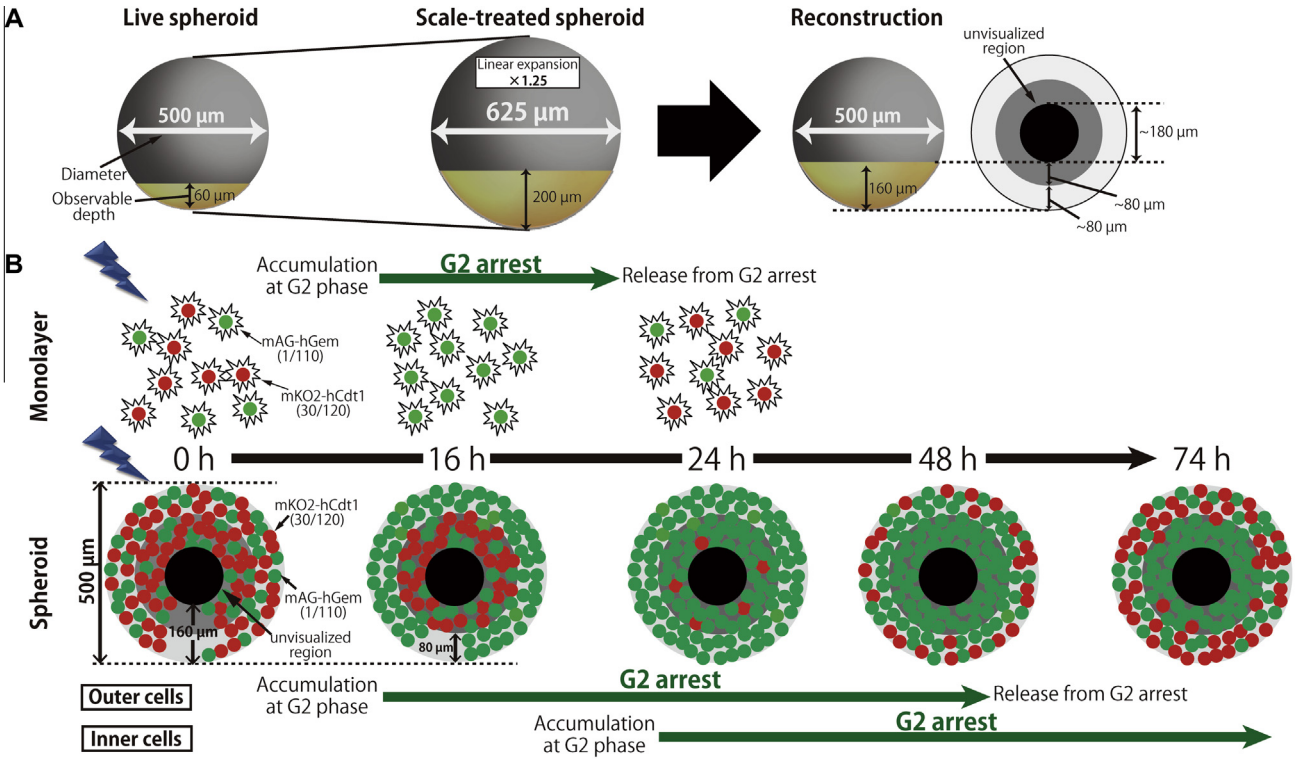

Fig. 4. Illustration of cell-cycle kinetics in HeLa-Fucci cells in the spheroid after 10-Gy irradiation. (A) Size and observable depth in a spheroid before and after Sca*l*e treatment. Reconstruction of the size of proliferating and dormant cell fractions at the equatorial plane in an original spheroid with a diameter of ~500 μm, based on geometrical calculations (assuming 1.25× expansion following Sca*l*e treatment) performed on the images in Fig. 3. Black circle: unvisualized region. (B) Summary of cell-cycle kinetics in HeLa-Fucci cells in monolayer culture and spheroids after irradiation. Green and red circles indicate the nuclei in S/G2/M and G1 cells, respectively. (For interpretation of the references to colour in this figure legend, the reader is referred to the web version of this article.)

the outer cells in the spheroid were accidentally attached to the agar surface of a culture dish at an early stage after irradiation, mitotic and red cells appeared more rapidly in the adherent outer layer than in the inner region (Supplementary Fig. 1). We reasoned that the loss of the tumor microenvironment resulting from attachment to the dish accelerated release from the G2 arrest.

3.3. Cell-cycle kinetics at inner positions in scale-treated spheroids after irradiation

It was difficult to sufficiently observe fluorescence kinetics in live spheroids at depths greater than 60 μm. To address this technical challenge, we applied Sca*l*e, an aqueous reagent that renders biological samples optically transparent, in order to reveal fluorescence kinetics at deeper positions in the spheroid. Following Sca*l*e treatment, we could observe at depths up to 200 μm, although the samples had to first be fixed in PFA [16]. Even at the observable limit, depth of 200 μm, the localization pattern of red and green was essentially the same as in the outer positions (Fig. 3 and 0 h). At the outer positions, 50 and 100 μm, fluorescence kinetics following irradiation was the same as in the live imaging. Interestingly, quite a few red fluorescent cells were identified 16 h after irradiation in the inner fraction, at depths of 150 and 200 μm, which were undetectable in live spheroids (Fig. 3 and 16 h). The quantitative line-profile analysis supported the finding (Supplementary Fig. 2). Twenty-four hours after irradiation, the red cells began to exhibit green fluorescence and prolonged G2 arrest, as in the outer cells. Laurent et al. reported that a proliferation gradient exists within spheroids that depends on depth [9]; therefore, it is reasonable to interpret the inner red fraction as a quiescent G0 cell population. Cycling G1 cells with red fluorescence in the outer growth fraction promptly progressed and were arrested at G2 phase, whereas inner quiescent cells were maintained in G0 phase for some time; this may explain why the contrast was visualized at the deep position. Presumably, some microenvironmental changes occurring after irradiation caused recruitment of the quiescent cells into the cycling phase; subsequently, the red cells turned green and again exhibited prolonged G2 arrest, similar to cells in the outer fraction. It should be noted that this system clearly captured the drastic radiation-induced change from the predominantly red fluorescence in all observable regions within the spheroid (Fig. 3 and 0 h), which veiled the distinction between the inner and outer regions.

In the Sca*l*e-treated spheroid 16 h after irradiation, the distance to the outermost red fraction from the surface was ~110 μm at the depth of 200 μm obtained in the confocal image (Fig. 3). Considering that samples expand linearly ~1.25-fold after Sca*l*e treatment [16], the red fraction was more than 80 μm below surface at the equatorial plane in the original spheroid, as revealed by a geometrical calculation from measurements at the confocal plane (Fig. 4A). Fig. 4B shows a summary of the differences in the cell-cycle kinetics of the outer and the inner fractions in a reconstructed original spheroid with a diameter of ~500 μm.

In this study, we used the Fucci system to visualize for the first time the cell-cycle kinetics in spheroids after irradiation without histological preparation. Fluorescence was detectable only up to depths of up to 60 μm in live spheroids; however, using the Sca*l*e treatment, we could observe fluorescence at depths up to 160 μm (original size), although unvisualized regions still persisted near the center (Fig. 4A and B); it is possible that tumor spheroids are more refractory to Sca*l*e-induced transparency than mouse embryos or neural tissues [16]. Recently, two groups described cell-cycle kinetics visualized by applying Fucci to spheroid models [9,17]. Those authors used spheroids consisting of tumor cells,

expressing either a red or green probe, and prepared as thin sections. In those studies, the cell-cycle transition was not clearly detectable, due to the use of a single probe, and the cell density in the thin sections was insufficient to obtain clear images. Our novel approach overcame such problems, leading to clear and convincing images. It still remains unclear which microenvironmental factors, potentially including oxygen tension, caused the prolongation of G2 arrest after irradiation observed in this study. Merely providing an anchorage-independent growth condition is unlikely to be sufficient to obtain such a phenotype (Supplementary Fig. 3). Further studies will be necessary to resolve the mechanisms of the prolonged G2 arrest in the spheroids. In such efforts, our novel method will be a useful tool for analyzing the effects of tumor microenvironments on tumor cell-cycle kinetics following DNA damage.

Acknowledgments

The authors thank Dr. A. Miyawaki and Dr. A. Sakaue-Sawano for providing the HeLa cells expressing the Fucci probes. A.K is a JSPS Research Fellow, and this study was supported in part by Grants-in-Aid for Scientific Research from MEXT and JSPS (252855, 23390427, and 25670798) to A.K. and M.M.

Appendix A. Supplementary data

Supplementary data associated with this article can be found, in the online version, at http://dx.doi.org/10.1016/j.bbrc.2013.08.093.

References

[1] D. Hanahan, R.A. Weinberg, Hallmarks of cancer: the next generation, Cell 144 (2011) 646–674.
[2] H. Harada, M. Inoue, S. Itasaka, K. Hirota, A. Morinibu, K. Shinomiya, L. Zeng, G. Ou, Y. Zhu, M. Yoshimura, W.G. McKenna, R.J. Muschel, M. Hiraoka, Cancer cells that survive radiation therapy acquire HIF-1 activity and translocate towards tumour blood vessels, Nat. Commun. 17 (2012) 783.
[3] R.E. Durand, J.A. Raleigh, Identification of nonproliferating but viable hypoxic tumor cells in vivo, Cancer Res. 58 (1998) 3547–3550.
[4] E. Sham, R.E. Durand, Cell kinetics and repopulation parameters of irradiated xenograft tumours in SCID mice: comparison of two dose-fractionation regimens, Eur. J. Cancer 35 (1999) 850–858.
[5] L.C. Kimlin, G. Casagrande, V.M. Virador, In vitro three-dimensional (3D) models in cancer research: an update, Mol. Carcinog. 52 (2013) 167–182.
[6] E.J. Hall, J. Giaccia, Spheroids: An *In Vitro* Model Tumor System, Radiobiology for the Radiologist, seventh ed., Lippincott Williams & Wilkins, Philadelphia, 2012. pp. 365–367.
[7] V. Lobjois, C. Frongia, S. Jozan, I. Truchet, A. Valette, Cell cycle and apoptotic effects of SAHA are regulated by the cellular microenvironment in HCT116 multicellular tumour spheroids, Eur. J. Cancer 45 (2009) 2402–2411.
[8] F. Hirschhaeuser, H. Menne, C. Dittfeld, J. West, W. Mueller-Klieser, L.A. Kunz-Schughart, Multicellular tumor spheroids: an underestimated tool is catching up again, J. Biotechnol. 148 (2010) 3–15.
[9] J. Laurent, C. Frongia, M. Cazales, O. Mondesert, B. Ducommun, V. Lobjois, Multicellular tumor spheroid models to explore cell cycle checkpoints in 3D, BMC cancer 13 (2013) 73.
[10] N. Motoyama, K. Naka, DNA damage tumor suppressor genes and genomic instability, Curr. Opini. Genet. Dev. 14 (2004) 11–16.
[11] T. Tamamoto, K. Ohnishi, A. Takahashi, X. Wang, H. Yosimura, H. Ohishi, H. Uchida, T. Ohnishi, Correlation between gamma-ray-induced G2 arrest and radioresistance in two human cancer cells, Int. J. Radiat. Oncol., Biol., Phys. 44 (1999) 905–909.
[12] M. Ishikawa, Y. Ogihara, M. Miura, Visualization of radiation-induced cell cycle-associated events in tumor cells expressing the fusion protein of Azami Green and the destruction box of human Geminin, Biochem. Biophys. Res. Commun. 389 (2009) 426–430.
[13] A. Kaida, N. Sawai, K. Sakaguchi, M. Miura, Fluorescence kinetics in HeLa cells after treatment with cell cycle arrest inducers visualized with Fucci (fluorescent ubiquitination-based cell cycle indicator), Cell Biol. Int. 35 (2011) 359–363.
[14] A. Kaida, M. Miura, Visualizing the effect of hypoxia on fluorescence kinetics in living HeLa cells using the fluorescent ubiquitination-based cell cycle indicator (Fucci), Exp. Cell Res. 318 (2012) 288–297.
[15] A. Sakaue-Sawano, H. Kurokawa, T. Morimura, A. Hanyu, H. Hama, H. Osawa, S. Kashiwagi, K. Fukami, T. Miyata, H. Miyoshi, T. Imamura, M. Ogawa, H. Masai, A. Miyawaki, Visualizing spatiotemporal dynamics of multicellular cell-cycle progression, Cell 132 (2008) 487–498.
[16] H. Hama, H. Kurokawa, H. Kawano, R. Ando, T. Shimogori, H. Noda, K. Fukami, A. Sakaue-Sawano, A. Miyawaki, Scale: a chemical approach for fluorescence imaging and reconstruction of transparent mouse brain, Nat. Neurosci. 14 (2011) 1481–1488.
[17] I. Dufau, C. Frongia, F. Sicard, L. Dedieu, P. Cordelier, F. Ausseil, B. Ducommun, A. Valette, Multicellular tumor spheroid model to evaluate spatio-temporal dynamics effect of chemotherapeutics: application to the gemcitabine/CHK1 inhibitor combination in pancreatic cancer, BMC Cancer 12 (2012) 15.